J Electroceram (2012) 28:118–122
DOI 10.1007/s10832-012-9691-x

Mechanism analysis and output characteristics experiments of an ultrasonic motor with circumferential surface drive

Hui Guo · Junhua Yao · Xunbo Li · Huafeng Li

Received: 19 November 2009 / Accepted: 9 February 2012 / Published online: 21 February 2012

Abstract A kind of ultrasonic motor, whose rotor is driven by stator's inner circumferential surface, has been designed and fabricated. The paper has analyzed the stator deformation characteristics under bending mode by using finite element method, identified the motor's working mechanism with two-phase voltage drive, and studied the different functions of tangential and radial displacements of the stator's inner circumference small teeth under bending mode and pointed that the above mentioned displacements along two directions of small teeth could drive the rotor continuously with single-phase voltage. The paper has discussed the motor's rotary direction reversing and put forward a concrete scheme of reversing with single-phase voltage drive. The mode of the stator was obtained by experiment. Under two-phase and single-phase voltages, running experiments of the motor have been accomplished and the corresponding characteristics curves have been drawn. Taken above analysis result as driving mechanism, a kind of thin-type standing ultrasonic motor can be developed further.

Keywords Ultrasonic motor · Stator · Tooth · Displacement · Drive with single-phase voltage

H. Guo (✉) · J. Yao · X. Li
School of Mechatronics Engineering,
University of Electronic Science and Technology of China,
Chengdu 610054, China
e-mail: hnrguohui@yahoo.com.cn

H. Li
Research Center of Ultrasonic Motors,
Nanjing University of Aeronautics & Astronautics,
Nanjing 210016, China

1 Introduction

The ultrasonic motor utilizes the piezoelectric effect to make the stator generate high-frequency vibration, and then rely on the friction between the stator and rotor to drive the rotor, the working principle is different from that of traditional electromagnetic motors. The ultrasonic motor has been used in autofocus system, robot and medical equipment.

In recent years, new progress has been made in the research on annular piezoelectric ultrasonic motors. In terms of driving mechanism, Reference [1] introduced a way to drive the motor by utilizing the phase difference of two traveling-waves. Reference [2] developed a new kind of annular standing wave ultrasonic motor, whose stator was designed into the shape of cymbal to convert the vibration mode, and the rotor has three fins to realize the rotation of the motor. Reference[3]based on shear-shear mode to excite the bending traveling wave. The corresponding prototype was constructed and characterized. Reference [4] focused on the motors miniaturization, presented circular plate rotary motor with 1,000 μm diameter, and completed micro-gear driving experiment on the motor. Reference [5] put forward a kind of rotary motor with multi-degree of freedom by utilizing the annular stator's radial and bending modes. Regarding the application of the motor, Reference [6] and [7] researched annular motors used in low-temperature environment and robot arms respectively.

In the above mentioned research, the bending mode of annular stator was used to drive the rotor. Reference[8] and [9] developed another kind of annular piezoelectric ultrasonic which used the non-axisymmetric mode of annular stator, and the contact part of stator and rotor was inner or outer circumference side of the stator. Such motor can effectively reduce the motor's thickness and miniaturize the product. But the non-axisymmetric mode of the annular stator is not easy to excite. Reference[10] developed a new

type of ultrasonic motor, and its characteristic was that the middle part of the round stator was shaped into windmill holes and the rotor was installed in the special-shaped hole of the stator. The deformation of the special-shaped hole under non-axisymmetric mode was used to rotate the rotor. In this paper, we used stator's bending mode to drive the rotor of the piezoelectric ultrasonic motor, referred to the structural characteristics of non-axisymmetric mode motor, and changed the contact interface of stator and rotor. Experiments proved that the reform made the motor still run normally only with single-phase alternating voltage. The working mechanism has been analyzed in this paper. The actual prototype motor's running experiments have been completed, and experiment results have been obtained. On the basis of above working mechanism analysis and prototype motor's running test, a new standing wave rotary ultrasonic motor can be developed.

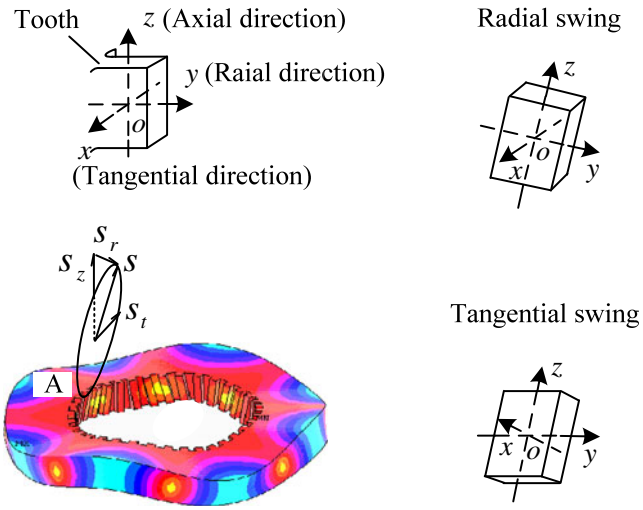

Fig. 2 B_{04} mode shape of the stator and displacement of the small tooth

2 Driving mechanism analysis

Figure 1 shows the structure of experimental prototype motor, the stator consists of ring steel sheet and ring-shaped piezoelectric ceramic, and they are bonded together. The small teeth are uniformly distributed along the inner ring. The rotor is a stepped short-axis, and its one end is installed in the stator's central hole. Size of the stator is as following: for the ring steel sheet: outer diameter 46 mm, inner diameter 26 mm, thickness 5.9 mm, and for the piezoelectric ceramic ring: outer diameter 45 mm, inner diameter 30 mm, thickness 0.4 mm.

In order to identify the motor's working mechanism, the paper has made mode analysis of the stator by using finite element method. The calculation result shows that at the frequency of 46.39 kHz the stator has bending mode B_{04}, and its vibration mode shape is shown in the left part of Fig. 2. The figure shows that the displacement of each small tooth has three components: respectively along radial, tangential and axial directions, the radial and the axial displacements are shown in the right part of Fig. 2. Because of the radial displacement, when a traveling-wave is excited on the stator,

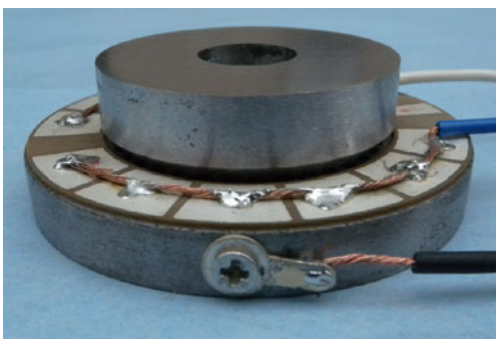

Fig. 1 Structure of the motor

the elliptical motion trajectories of the stator particles get to lean. For example, to point A, S_r is the radial displacement and S_z is the axial displacement, and the two displacement components synthesize S, while S and the tangential displacement S_t synthesize, then an elliptical motion trajectories can formed. Radial displacement S_r result in an angle between the elliptical motion trajectories and vertical surface, such leaning enables the stator's inner ring to drive the rotor. So the motor can run normally with two-phase voltage.

The bending mode shown in Fig. 2 is excited on stator when the stator is applied with single-phase voltage. Because the small teeth of the stator swing along radial direction, the stator contacts with the rotor only at wave crest and wave trough. At this moment, only the eight small teeth near the wave crest or the wave trough are possible to rotate the rotor, so in order to analyze driving mechanism with single-phase voltage, we only need to discuss the motion trajectories of above mentioned small teeth. To visually represent the teeth driving effect on the rotor, we spread out the stator inner ring to a plane, and then show the displacement variation of the small teeth during one period in Fig. 3. In the figure, black-painted part stands for the radial swing pointed to axis and no black-painted part stands for the radial swing deviated away from axis so to clearly illustrate the radial swing of the teeth.

We assume that vibration period of B_{04} mode is T and the time is t, shown in Fig. 3.

When $t=0$, the tangential and radial displacements of the eight small teeth are zero, so the rotor is in a static state.

When $0 < t < T/4$, the ring stator's B_{04} mode is excited, small teeth 1, 3, 5, 7 swing anticlockwise along the tangential direction, meanwhile, the tops of teeth 1, 3, 5, 7 produce radial displacements pointed to the axis and contact with the rotor, while the bottoms of these teeth produce displacements

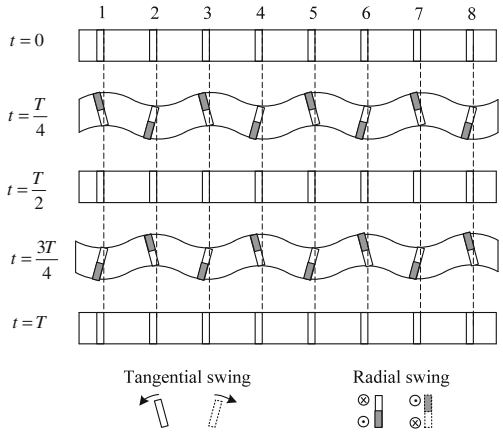

Fig. 3 Stator teeth displacements in one period

deviated from the axis and do not contact with the rotor. Therefore, small teeth 1, 3, 5, 7 rotate the rotor to the left. Small teeth 2, 4, 6, 8 swing clockwise along the tangential direction, and the tops of these teeth produce displacements deviated from the axis and do not contact with the rotor. And the bottoms of these teeth produce displacements pointed to the axis and contact with the rotor, so teeth 2, 4, 6, 8 can also drive the rotor to the left.

When t = T/4, small teeth 1~8 reach their respective maximum displacements.

When T/4 < t < T/2, small teeth 1,3,5,7 swing clockwise along the tangential direction, and the tops of small teeth 1, 3, 5, 7 produce the radial displacements deviated from the axis, so they cannot drive the rotor. And the bottoms of small teeth 1,3,5,7 produce the displacements pointed to the axis, but do not yet contact with the rotor, so they cannot rotate the rotor. In a similar way, although small teeth 2, 4, 6, 8 swing anticlockwise along the tangential direction, both of the tops and bottoms of small teeth 2, 4, 6, 8 do not contact with the rotor, therefore, they cannot drive the rotor either.

When t = T/2, the tangential and radial displacements of all small teeth are zero, and all the small teeth return to their respective equilibrium positions.

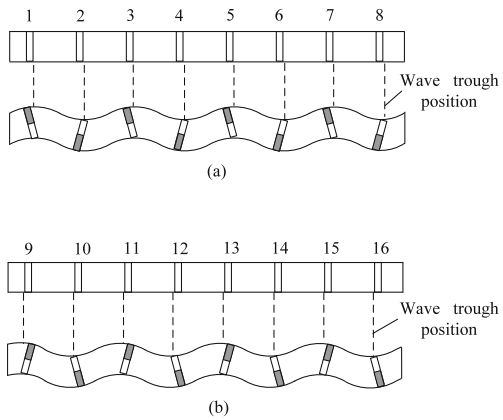

Fig. 4 Mechanism of the motor reversing

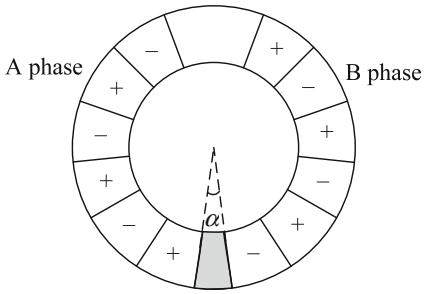

Fig. 5 Electrode arrangement of the piezoelectric ceramic

When T/2 < t <3T/4, small teeth 1, 3, 5, 7 swing clockwise along the tangential direction, the tops of teeth 1, 3, 5,7 produce the radial displacements deviated from the axis, so they cannot drive the rotor. And the bottoms of these teeth produce radial displacements pointed to the axis and get to contact with the rotor, so they can drive the rotor to the left. Small teeth 2, 4, 6, 8 swing anticlockwise along the tangential direction, the tops of these teeth produce displacements pointed to the axis and get to contact with the rotor, so the rotor can be driven to the left.

When t = 3T/4, small teeth 1~8 reach their respective maximum displacements, but the swing direction is quite contrary to that when t = T/4.

When 3T/4 < t < T, small teeth 1, 3, 5, 7 swing anticlockwise along the tangential direction, the tops of the teeth produce displacements pointed to the axis, but do not yet contact with the rotor, the bottoms of the teeth deviate from the axis, therefore, these teeth cannot drive the rotor. Similarly, small teeth 2, 4, 6, 8 cannot drive the rotor either.

When t = T, the tangential and radial displacements of all small teeth are zero, and all small teeth return to their respective equilibrium positions.

Through one-period motion analysis of eight small teeth, we know that when the stator is excited with single-phase voltage, the radial and tangential motions of these eight small teeth in the stator's inner ring can rotate the motor's

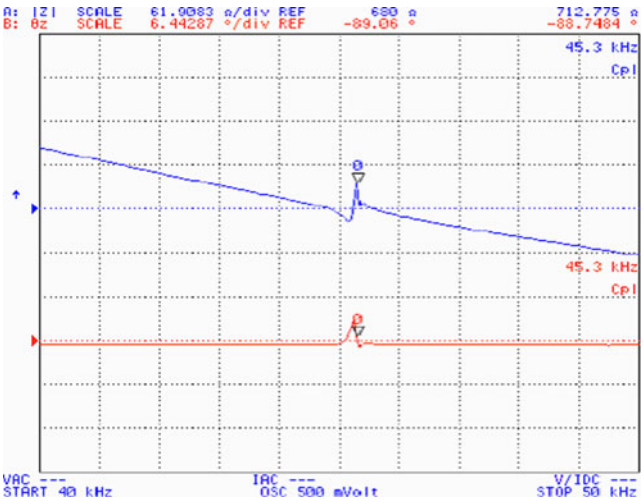

Fig. 6 Piezoelectric impedance curve of the stator

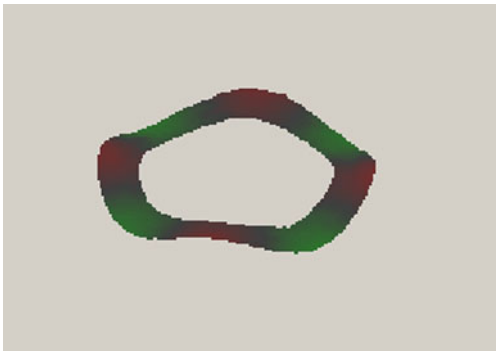

Fig. 7 Mode shape of the stator by laser Doppler vibrometer

rotor along a fixed direction. Because the tangential swing directions of the small teeth determine the rotary direction of the rotor, we can change the rotary direction of the motor by changing tangential swing directions of the small teeth. Figure 4 illustrates the reversing mechanism, Fig. 4(a) shows that the wave crest and the wave trough after stator's deformation are located on the right sides of the eight small teeth 1~8. When $0 < t < T/4$, the tops of small teeth 1, 3, 5, 7 and the bottoms of small teeth 2, 4, 6, 8 drive the rotor to the left. While Fig. 4(b) shows that the wave crest and the wave trough after stator's deformation are located on the left sides of the eight small teeth 9~16. and when $0 < t < T/4$, the tops of small teeth 9, 11, 13, 15 and the bottoms of small teeth 10, 12, 14, 16 drive the rotor to the right. In Fig. 4(a) and (b), the bending modes of the stator are same but the locations of the wave crest or the wave trough are different. The bending mode of the stator is excited by piezoelectric ceramic which are bonded to the stator, the location changes of wave crest and trough can be realized by special electrode arrangement of piezoelectric ceramic. In the piezoelectric ceramic as Fig. 5, the two phases of A and B are separated from each other. Adjusting the phase angle α between Phase A and B can make the wave crest after stator deformation respectively located on the left side and the right side of small teeth when A phase or B phase is applied, as Fig. 4.

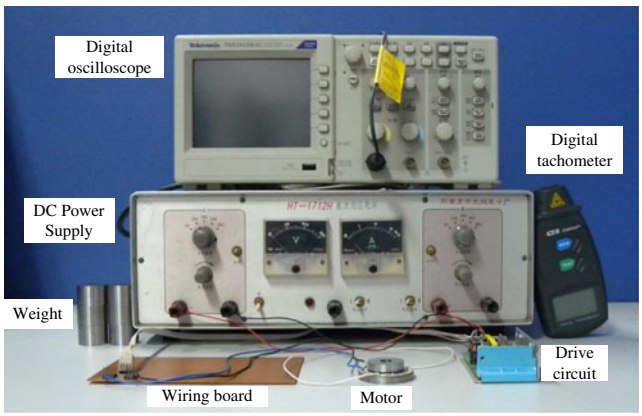

Fig. 8 Running test device of the motor

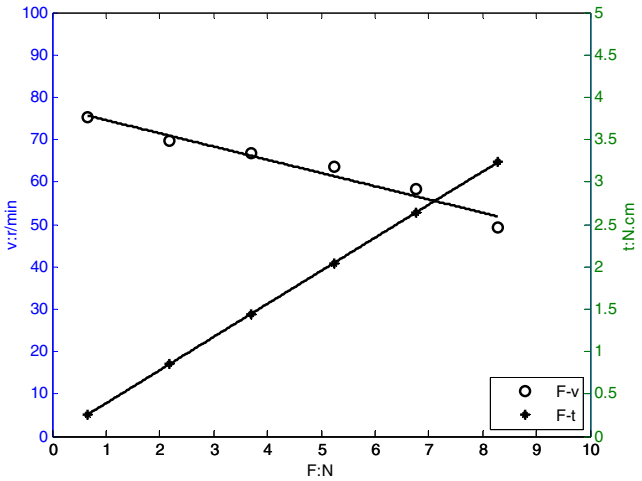

Fig. 9 Characteristics of pre-tightening force versus speed and pre-tightening force versus torque with single-phase voltage

According to the above commutating mechanism, reversing the motor can be achieved, and the experiment confirms that the motor can run positively and reversely.

3 Driving experiments

In order to verify the calculation result of finite element method, we have done following tasks: First, we have used precision impedance analyzer of Agilent 4294A and measured the piezoelectric impedance curve of the stator. In the experiment, AC voltage with variable frequency output by the impedance analyzer is applied on the stator to excite the piezoelectric ceramic and deform piezoelectric ceramic so to cause the vibration of the stator. Because the piezoelectric ceramics has piezoelectric effect, therefore, the mechanical resonance frequency of the stator can be obtained according

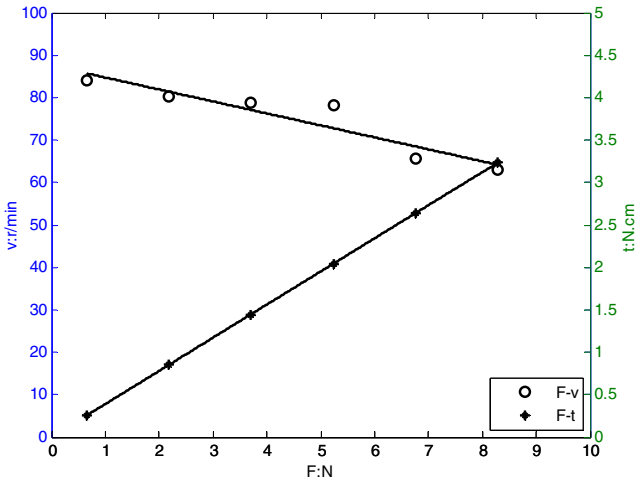

Fig. 10 Characteristics of pre-tightening force versus speed and pre-tightening force versus torque with two phase voltage

to piezoelectric impedance curve. Figure 6 indicates the piezoelectric impedance experimental curve, the vertical axis is the magnitude of the impedance and the horizontal axis is the frequency of input voltage signal. From this figure we can learn that there is a peak of the impedance magnitude near the frequency of 45.3 kHz, we determine that the mechanical resonance frequency of the stator exist near the 45.3 kHz, which conforms to the calculation result of finite element method. Secondly, we have used laser Doppler vibrometer PVS-300F and tested the vibration mode of the stator. Figure 7 shows the mode shape of the stator at the frequency of 45.22 kHz. So the experiment result is consistent with the calculation result in Fig. 2. In addition, we have done the running experiments on the prototype motor with single-phase voltage and two-phase voltage. The test device consists of DC power supply, digital oscilloscope, tachometer, piezoelectric drive circuit and home-made weights, shown in Fig. 8. The direct current voltage of 12 V provided by the DC power supply is connected with piezoelectric driving circuit, where the alternating current voltage is output on the prototype. The digital oscilloscope is used to measure frequency of the alternating current voltage, and tachometer is used to measure rotary speed of the motor. In due order home-made weights are added on the rotor to adjust the frictional force and pre-tightening force between the stator and the rotor. We write down figures of weights and motor's rotary speeds, based on that, relationships between pre-tightening force and rotary speed, pre-tightening force and rotary torque are characterized. The corresponding experimental data and the fitting curve with single-phase driving voltage and two-phase driving voltage are shown in Figs. 9 and 10 respectively. According to the experiments, the output characteristic is related to two factors: performance of drive circuit and the quality of silver-plated surface of piezoelectric ceramic. If we improve the two factors, the motor's torque and speed are enhanced significantly.

4 Conclusion

This paper has put forward a thin-type ultrasonic motor, analyzed two different driving mechanisms and completed running experiment. The feasibility of the two driving modes has been verified. The motor can function properly in two driving modes, so it can present different output torques, and the application scope of the motor can be enlarged. In addition, the motor also has a simple structure. The key problems to improve the output characteristics of the motor are: ensure quality of the silver-plated surface of piezoelectric ceramic to enhance the performance of drive circuit; ensure stability of the waveform and the frequency of the output voltage. Further work includes improvement on electrode arrangement of piezoelectric ceramic and using outer circumferential side of the stator to drive the rotor.

References

1. D. Bai, T. Ishii, K. Nakamura, S. Ueha, T. Yonezawa, T. Takahashi, An ultrasonic motor driven by the phase-velocity difference between two traveling waves. [J] IEEE Trans. Ultrason. Ferroelectrics. Freq. Contr. **51**(6), 680–685 (2004)
2. J.T. Leinvuo, S.A. Wilson, R.W. Whatmore, M.G. Cain, A new flextensional piezoelectric ultrasonic motor-design, fabrication and characterization. Sensor Actuator A **133**, 141–151 (2007)
3. S. Dong, J. Zhang, H.W. Kim, M.T. Strauss, K. Uchino, D. Viehland, Flexural traveling wave excitation based on shear-shear mode. [J] IEEE Trans. Ultrason. Ferroelectrics. Freq. Contr. **51**(10), 1240–1245 (2004)
4. V. Kaajakari, A. Lal, Micromachined ultrasonic motor based on parametric polycrystalline silicon plate excitation. [J] Sensor Actuator A **137**, 120–128 (2007)
5. S. Dong, L. Yan, D. Viehland, A piezoelectric single crystal traveling wave step motor for low-temperature application. [J] Appl. Phys. Lett. **92**, 153504-1–153504-3 (2008)
6. J.-S. Rho, K.-I. Oh, H.-S. Kim, H.-K. Jung, Characteristic analysis and design of a B14 roatry ultrasonic motor for a robot arm taking the contact mechanism into consideration. [J] IEEE Trans. Ultrason. Ferroelectrics. Freq. Contr. **54**(4), 715–728 (2007)
7. T. Takano, H. Hirata, Y. Tomikawa, Analysis of nonaxisymmetric vibration mode piezoelectric annular plate and its application to an ultrasonic motor. [J] IEEE Trans. Ultrason. Ferroelectrics. Freq. Contr. **37**(6), 558–565 (1990)
8. L. Lebrun, L. Petit, P. Gonnard, Piezoelectric motor using a (1,1) non-axisymmetric mode. [J] Ultrasonics **34**, 251–255 (1996)
9. M. Aoyaagi, T. Nakajima, Examination of disk-type multidegree-of-freedom ultrasonic motor. Jpn. J. Appl. Phys. **43**(5B), 2884–2890 (2004)
10. C.-B. Yoon, S.-M. Lee, H.-E. Kim, K.-W. Lee, Windmill-type ultrasonic micromotor fabricated by thermoplastic green machining process. [J] Sensor Actuator A **134**, 519–524 (2007)